



PHOTOCONDUCTIVITY EFFECTS IN AIR-INDUCED AND FLUOROFULLERENE-INDUCED SURFACE CONDUCTING DIAMOND

Fadhlia Zafarina Zakaria

Department of Physics, School of Fundamental Sciences, Universiti Malaysia Terengganu, Kuala Terengganu, Malaysia

E-Mail: fadhlia@umt.edu.my

ABSTRACT

The photoelectrical properties of the hydrogen-terminated diamond surface in the presence of a surface conducting layer have not been reported in the literature. This paper presents a preliminary study of the photoelectrical behaviour of the air-induced and fluorofullerene-induced surface conducting diamond. The photoconductivity observed is attributed to the excitation of electrons from the near-surface valence band into trap states, giving rise to a higher sub-surface hole current. A photocurrent buildup was observed upon laser exposure, with the highest photocurrent up to 56% higher than the initial (dark) current at the diamond surface in the case of doping with $C_{60}F_{48}$. This appears to be considerably higher than the same sample when doped with water. The observed behaviour suggests a possible influence on the level of photoconductivity due to the nature of the acceptor layer, but may alternatively reflect a trend that a reduced (dark) surface conductivity results in a higher relative increase in the photocurrent when exposed to light. The subsequent persistent decay of the photocurrent suggests the role of charge trapping at the trap states. The decay of the photoconductivity takes the form of a stretched exponential typical of a persistent photoconductivity, with the decay exponent, β values found to be below 0.4 and the decay constants in the range of 46-286 s.

Keywords: photoconductivity, persistent photoconductivity, surface conducting diamond, stretched exponential decay.

1. INTRODUCTION

The wide bandgap (5.47 eV) characteristic of diamond has made it an extremely special semiconductor with astonishing electronic and optical properties. Diamond prepared by chemical vapour deposition (CVD) methods can produce high-quality single crystal material which has the desired properties for fabrication of numerous electronic devices [1]. Hydrogen-termination of diamond in a hydrogen plasma yields a surface with negative electron affinity of typically -1.3 eV and an ionization potential of 4.2 eV, which is low compared to other semiconductors [2]. A clean C(100) surface forms a 2x1 reconstruction with C-C double bonded dimers [3, 4]. The double bond dimer is transformed to a single bond upon H-termination with each carbon atom attached to one H-atom [5].

Diamond is an insulator if undoped[6]. Ordinary bulk doping incorporates atomic dopants into the host lattice of diamond using an appropriate acceptor or donor, such as boron doping to produce a *p*-type conductivity and nitrogen or phosphorous doping to produce an *n*-type conductivity [1]. In contrast, surface transfer doping can occur when a water layer serving as the acceptor comes in contact with H-terminated diamond surface as a result of air exposure. In this type of doping, the reduced ionization potential of the H-terminated diamond surface and the presence of a high electron affinity adsorbate layer mutually contribute to the surface conductivity through surface transfer doping [6].

This process is possible due to the fact that the lowest unoccupied level of the acceptor layer resides lower than the valence band maximum, VBM of the diamond, triggering the movement of electrons from the

diamond valence band into the empty electronic states of the acceptor layer leaving holes confined to the diamond surface which caused an upward band bending and the rise of *p*-type surface conductivity [6]. Other molecular acceptors with sufficiently high electron affinities capable of providing a considerable high doping concentration on H-terminated diamond surface are fullerene (C_{60}), fluorinated fullerene ($C_{60}F_{48}$) and molybdenum trioxide (MoO_3), demonstrating hole sheet densities up to $1 \times 10^{14} \text{ cm}^{-2}$ [7]. More recent surface acceptor oxides that have been explored on the H-terminated diamond are vanadium pentoxide, V_2O_5 [8], tungsten trioxide, WO_3 and rhenium trioxide, ReO_3 [9] which result in a hole carrier concentration of up to $2.52 \times 10^{14} \text{ cm}^{-2}$ on the surface conducting diamond.

Although studies of surface conducting diamond have progressed towards utilizing molecules as surface acceptors with the aim of developing more controllable and thermally stable doping as compared to water doping [7, 10], the influence of light on the surface conductivity has not been investigated and reported substantially. It is found that exposure to light can dramatically influence the conductivity and hole sheet density of the surface conducting channel. However, this effect has, to date, not been quantified nor is well understood. This paper aims to investigate the effect of light illumination on the air-induced and $C_{60}F_{48}$ -induced surface conductivity and presents a preliminary characterization of the photoconductivity effects observed.



2. EXPERIMENTAL DETAILS

2.1. Materials and procedures

The sample used for this measurement was a (100) orientated Ila commercial single-crystal diamond with four contacts in a van der Pauw geometry, fabricated with silver paint and connected to CuBe contacts on a cubic zirconium holder. For the air-induced surface conductivity, measurements are performed on an as-mounted diamond sample and after a one-hour anneal at 100°C in ultra-high vacuum (UHV). In-situ annealing of the sample was achieved using an electron-beam heater. In this case, the back plate of the sample holder was electron irradiated so that there is no irradiation of the sample surface. The fluorofullerene-doped surface was subsequently prepared using the same diamond, after annealing at 150°C for 24 hours to fully remove the water-induced conductivity. Prior to annealing, the sample has been pumped down in vacuum for many days which already reduced its conductivity. The resistance of the device were confirmed to be very high after annealing, consistent with the removal of adsorbate acceptors. Measurements were performed for two different C₆₀F₄₈ adlayers, deposited for 10 minutes and 30 minutes respectively from an in-situ sublimation source.

2.2. Photoconductivity measurements

In each case, photoconductivity measurements were performed with the sample mounted in vacuum. Prior to each measurement, the device was left in dark conditions overnight. The photoconductivity was induced using a green laser diode with the power of 1 mW, exposing the sample for 20 s. The wavelength of the light source was 532 nm, corresponding to a photon energy of 2.3 eV. The resulting sample current, with a voltage of 1V applied between two diagonal contacts across the sample, was monitored prior to, during, and subsequent to light exposure.

2.3. Fitting procedure

The photocurrent decay was fitted to a specific function so that the decay behaviour can be modelled and characteristic information about the decay extracted. The decay data are taken from the moment the light source was switched off in each case. Prior to fitting, the individual decay curves were normalized to unity at $t=0$ s, as shown in Figure 5. All decay curves were fitted from $t=0$ s to $t=5000$ s using the fitting procedures in Origin. All decay curves are fitted with the following stretched exponential function:

$$I(t) = I_0 e^{-\left(\frac{t}{\tau}\right)^\beta} + y_0 \quad (1)$$

where β is the decay exponent and τ is the decay time constant. $I(t)$ is the current at time t , and I_0 is the photocurrent directly after the laser illumination was terminated, defined as $t=0$ s.

3. RESULTS AND DISCUSSIONS

3.1. Photocurrent buildup

The growth of the sample current upon light exposure for the case of air-induced surface conductivity is shown in Figure-1. The dark current of the as-mounted diamond sample in UHV and after a one-hour anneal is 32.0 μ A and 8.0 μ A, respectively. The highest photocurrent observed for the two conditions after a 20 s period of light exposure is 33.0 μ A and 8.3 μ A. Therefore, the current increment from the (dark) steady state to the highest photocurrent reached are 3 and 4 % in each case.

After annealing in UHV, the dark current is four times lower than the as-mounted case. This variation reflects the reduction in density of water-based acceptors, and the concurrent reduction in underlying surface conductivity and hole sheet density, after the sample is annealed in vacuum. An additional effect of the reduced hole density would be an increase in the resistance of the metal contacts on the diamond surface which usually take the form of Schottky contacts, so the percentage increase in current resulting from light exposure, relative to the dark current, may more appropriately reflect the photocurrent excitation.

As noted earlier, the metal-diamond contacts behave as Schottky barriers and the contact resistance can decrease in response to charge accumulation in the diamond. As a result of annealing, the surface conductivity is removed from the channel and below the contacts. Annealing may also remove residual adsorbate below the metal contacts but there is no evidence for this mechanism taking place.

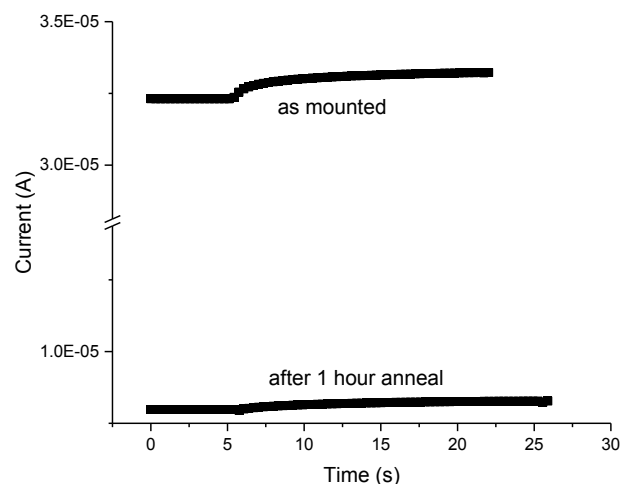


Figure-1. Current growth versus time on the as-mounted device in vacuum and after one hour of annealing in UHV.

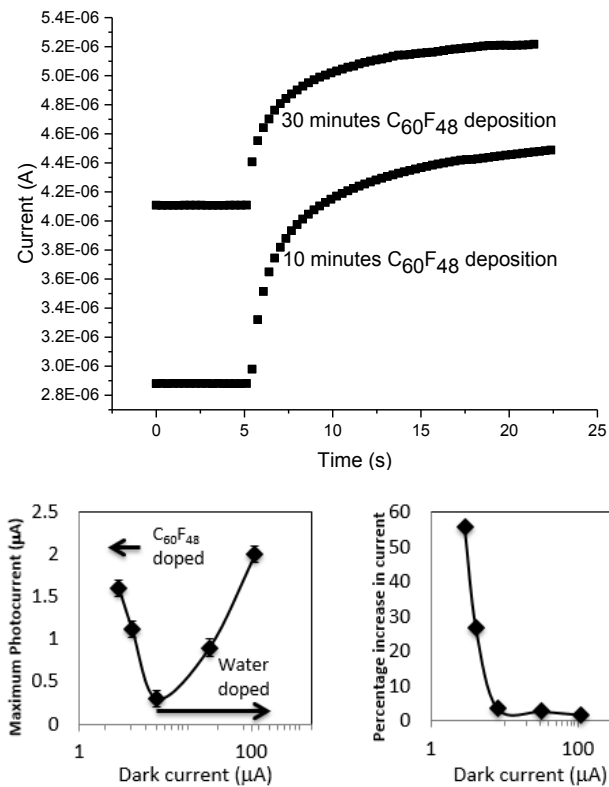


Figure-2. Photocurrent growth of air-induced and C₆₀F₄₈-induced surface conductivity on diamond (upper). The absolute and percentage increase in current as a result of laser exposure, as a function of the original sample dark current (lower).

The photocurrent buildup of the same sample when doped with C₆₀F₄₈ is shown in Figure-2. The constant current (up to 5 s) corresponds to the steady state dark current. As soon as the diamond device is illuminated with the green laser, the photocurrent similarly starts to rise until it reaches the highest value just before the laser is terminated (after a further 20 s). The dark current is lower than that observed for the same sample when doped with water. At first sight this seems unusual but most likely reflects the fact that the sample has been annealed overnight to remove water and the subsequent deposition rate of the fluorofullerene is very low so that the full initial level of surface conductivity is not recovered. However, the dark current measured for the sample after deposition of C₆₀F₄₈ for 30 minutes (4.1 µA) was found to be higher than that after deposition for just 10 minutes (2.9 µA), which suggests that the fluorofullerene is indeed doping the surface as expected but is present at a relatively low surface coverage. The sample is still relatively resistive after doping with C₆₀F₄₈ suggesting, in this case, that only a thin adsorbate layer has been added – compared to studies in the literature [11] that apply a monolayer or more of fluorofullerene.

The observed increase in current upon laser exposure, relative to the dark current, was determined to be 56 % in case of a 10 minute period of C₆₀F₄₈ deposition

and 27 % for the 30 minute deposition. These appear to be considerably higher than the same sample when doped with water. This is illustrated in the lower image of Figure 2, which gathers the percentage growth in current, relative to the dark current, for each of the doping scenarios described above plotted as a function of the dark current in each case. The observed behaviour suggests a possible influence on the level of photoconductivity due to the nature of the acceptor layer, but may alternatively reflect a trend that a reduced (dark) surface conductivity results in a higher relative increase in the photocurrent when exposed to light.

The thickness of the C₆₀F₄₈ layer could be controlled but in our case, this preliminary experiment is purposely carried out to show the light excitation effect on the C₆₀F₄₈-induced conductivity where the exact thickness of the layer was not particularly important at that stage, therefore, was not taken into account. The currents were recorded with a precision ammeter to ensure that small changes in current to the level of nA could be observed in samples that were highly resistive. The accuracy of the data is consistent with the precision of the measurement.

3.2. Photocurrent decay

Figure-3 shows the subsequent decay in photocurrent, upon termination of the laser source, for the sample as-mounted and after annealing in UHV. In each case, the highest photocurrent indicated on the graph corresponds to the current measured immediately prior to the termination of laser excitation. This data gives a clear indication that the photoconductivity is persistent in surface conducting diamond for several hours after termination of the light source. The photocurrent, measured here for over 2.5 hours after termination of the laser source, continues to decrease during this period.

Figure-4 shows the photocurrent decay for the same sample when doped with C₆₀F₄₈. As shown in the figure, and noted earlier, a longer deposition time results in a higher dark current. The photocurrent on the diamond surface in case of a C₆₀F₄₈ adlayer deposited for 30 minutes is 16 % higher than to that of 10 minutes deposition. The highest photocurrent prior to the termination of the laser illumination is 5.2 µA and 4.5 µA for the 30 minutes and 10 minutes, respectively. These values then decay slowly reaching 4.2 µA and 3.0 µA, respectively after a few hours. The result shows that the photocurrents have reduced by 19 % and 33 % during the decay process. These large changes reflect the corresponding dramatic increase in current when exposed to light, as shown in Figure-2.

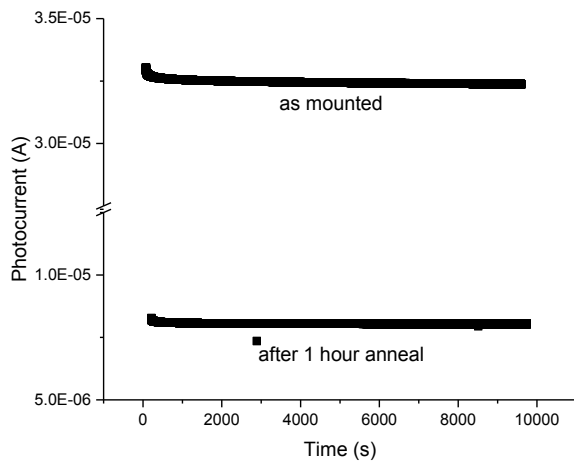


Figure-3. Photocurrent decay for the air-induced (as mounted diamond) and after annealing for an hour.

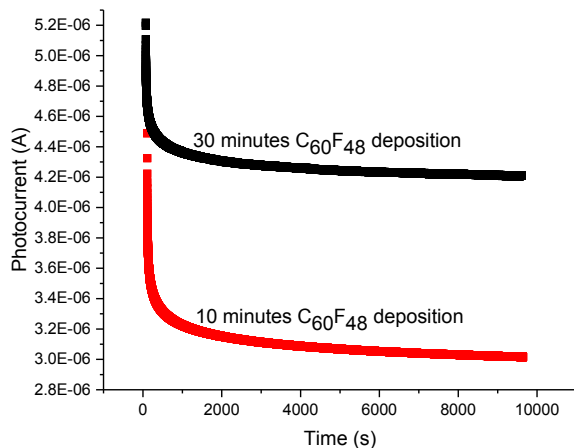
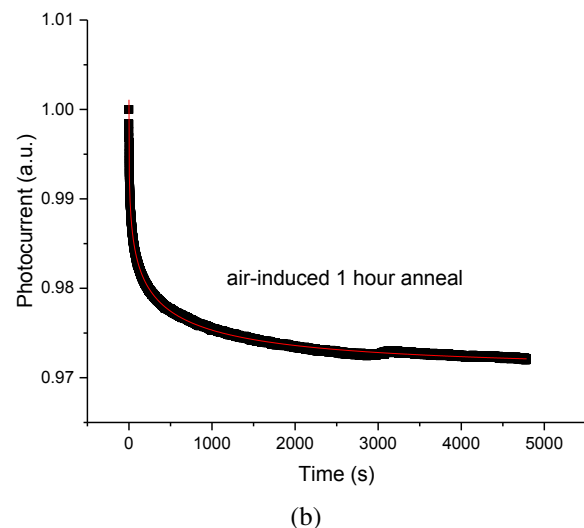
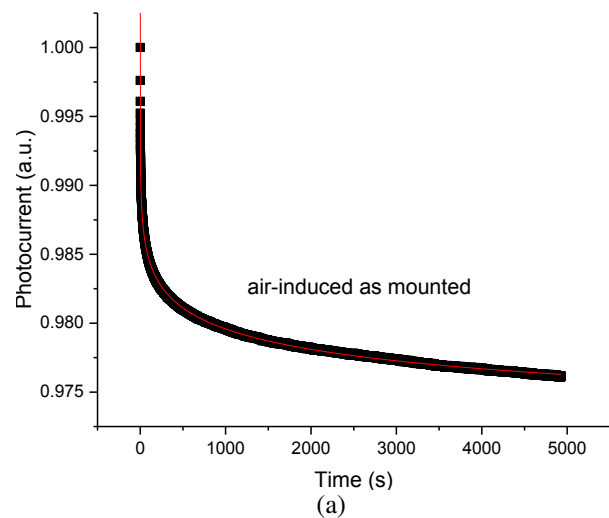


Figure-4. Photocurrent decay of $C_{60}F_{48}$ -induced surface conductivity of diamond following 10 and 30 minutes fluorofullerene deposition.

The level of photoconductivity observed, compared to that observed in the study of photoconductivity in bulk-doped diamond [12], and the fact that the nature and level of doping influence the achievable photoconductivity suggest that the photoexcitation of charge carriers occurs in the surface conducting layer at the hydrogen-terminated diamond surface. This may occur via the excitation of electrons from the near-surface valence band into trap states and we propose that the photocurrent observed arises predominantly from the generation of an increased hole current in the sub-surface accumulation layer. In this case, photoexcitation would occur for electrons at the Fermi level. At the highest levels of surface doping the Fermi level sits up to -0.8 eV below the valence band edge. As the doping level is reduced the Fermi energy increases, approaching and eventually exceeding the valence band maximum [13]. Photoexcitation at a fixed photon energy would therefore lead to electronic excitation across a range of gap states as the level of surface doping changes. The

subsequent decay of the photoconductivity, which takes the form of a stretched exponential typical of a persistent photoconductivity, similarly suggests the role of a band of charge trap states.

The photocurrent decay curves were normalized to unity at $t=0$ s and the data fitted to the stretched exponential function (equation 1). Figure-5 shows the fits on the normalized photocurrent decay curves versus time (to $t=5000$ s) for each type of doping condition. In each case the experimental data is represented by the black curve and the fitting line is represented by the red curve. It is evident from the plots that the decay data obtained from the experiment are well fitted by the decay function.



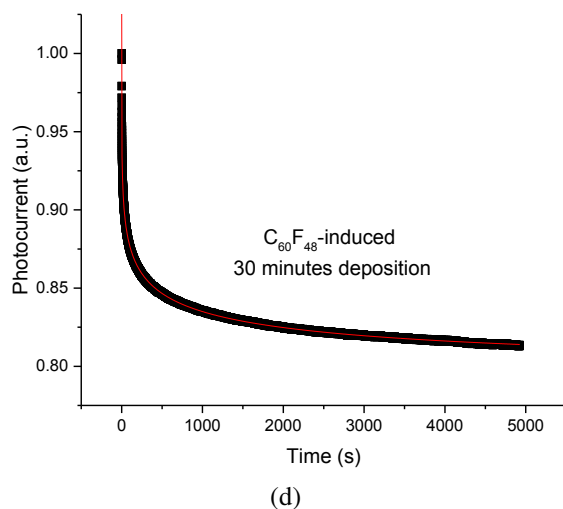
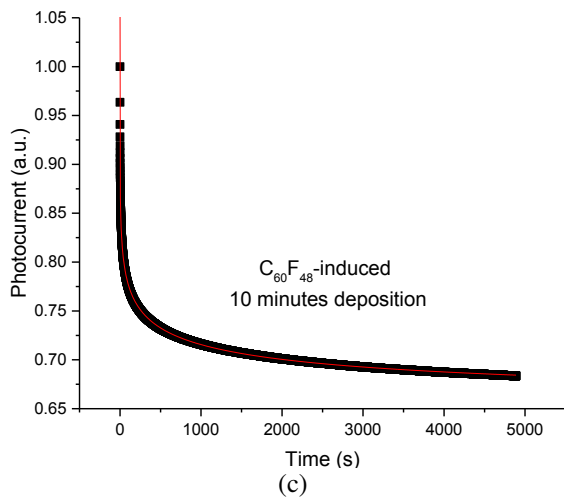


Figure-5. Normalized photocurrent decay at room temperature for various doping conditions on the H-terminated diamond (a) air-induced as mounted (b) air-induced after anneal (c) $C_{60}F_{48}$ -induced 10 minutes deposition (d) $C_{60}F_{48}$ -induced 30 minutes deposition. The black curve is the data while the red curve represents the fit.

Figure-6 shows the plot of the decay exponent, β versus the decay constant, τ derived from the stretched exponential fits. It is evident in the plot that the decay exponent is relatively constant between different doping conditions of the air-induced and fluorofullerene-induced surface photoconductivity except that the value is slightly higher for the annealed device via air exposure doping. The decay exponent, β of the as mounted sample is similar in value with the β of the $C_{60}F_{48}$ -induced doping. The β obtained for all cases are below 0.4 which show a highly stretched exponential decay characteristic corresponding to very low values. The highest value of the decay constant, τ (286 s) of the as mounted H-terminated diamond device corresponds to the highest dark and photocurrent values acquired. Similarly, the lowest decay time (46 s) of the device acquired via 10 minutes

$C_{60}F_{48}$ deposition presents the lowest obtained dark and photocurrent values. This preliminary study shows that the increase of the decay constant is consistent with the increase of the doping level on the surface conducting diamond.

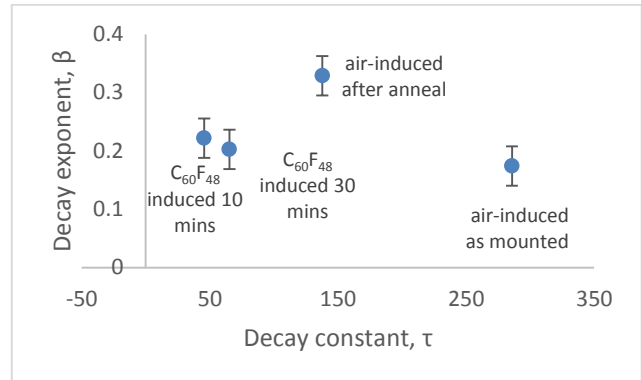


Figure-6. Plot of decay exponent versus decay constant showing the increment of the decay constant for different doping scenarios from doping with fluorofullerene towards doping with air exposure.

CONCLUSIONS

The photoconductivity behaviour of the air-induced and fluorofullerene-induced surface conducting hydrogen-terminated diamond in response to exposure with a 532 nm laser source were explored.

A photocurrent buildup was observed upon laser exposure, with the highest photocurrent up to 56% higher than the initial (dark) current at the diamond surface. The level of photocurrent achieved was found to be higher when the surface was doped with fluorofullerene compared to water doping, suggesting that the nature and doping level of the surface conducting layer influences the photoconductivity process.

In both doping scenarios a subsequent persistent decay of the photocurrent, lasting several hours, was observed upon termination of the laser source, suggesting the role of a range of charge trap states either at the diamond surface or in the acceptor layer.

The photocurrent decay curves were proven to be well fitted with the stretched exponential decay function. The decay exponents for both doping conditions were found to be below 0.4 which indicate a highly stretched exponential decay behaviour. The decay constants derived from the fits demonstrate the increase of the decay time from the $C_{60}F_{48}$ -induced towards the air-induced photoconductivity.

ACKNOWLEDGEMENTS

Author would like to thank Professor Chris Pakes, Eric Huwald and Robert Polglase from the Department of Chemistry and Physics, School of Molecular Sciences, La Trobe University, Victoria, Australia for their assistance. The author is grateful to



Universiti Malaysia Terengganu and Malaysia's Ministry of Higher Education for the scholarship provided.

REFERENCES

- [1] Wort C. J. H. and Balmer R.S. 2008. Diamond as an electronic Material. *Materials Today*. 11 (1-2): 22-28.
- [2] Ristein J. 2005. Diamond surfaces: familiar and amazing. *Applied Physics A*. 82(3): 377-384.
- [3] Wang Y. M., Wong K.W., Lee S.T., Nishitani-Gamo M., Sakaguchi I., Loh K.P. and Ando T. 2000. Recent studies on diamond surfaces. *Diamond and Related Materials*. 9 (9-10): 1582-1590.
- [4] Graupner R., Hollering M., Ziegler A., Ristein J., Ley L. and Stampfl A. 1997. Dispersions of surface states on diamond (100) and (111). *Physical Review B*. 55 (16): 10841-10847.
- [5] Furthmüller J., Hafner J. and Kresse G. 1996. Dimer reconstruction and electronic surface states on clean and hydrogenated diamond (100) surfaces. *Physical Review B*. 53 (11): 7334-7351.
- [6] Maier F., Riedel M., Mantel B., Ristein J. and Ley L. 2000. Origin of Surface Conductivity in Diamond. *Physical Review Letters*. 85(16): 3472-3475.
- [7] Tordjman M., Saguy C., Bolker A. and Kalish R. 2014. Superior Surface Transfer Doping of Diamond with MoO₃. *Advanced Materials Interfaces*. 1(3): 1300155- 13000160.
- [8] Crawford K.G., Cao L., Qi D., Tallaire A., Limiti E., Verona C., Wee A. T. S. and Moran D. A. J. 2016. Enhanced surface transfer doping of diamond by V₂O₅ with improved thermal stability. *Applied Physics Letters*. 108 (4): 042103.
- [9] Tordjman M., Weinfeld K. and Kalish R. 2017. Boosting surface charge-transfer doping efficiency and robustness of diamond with WO₃ and ReO₃. *Applied Physics Letters*. 111 (11): 111601.
- [10] Strobel P., Riedel M., Ristein J., Ley L. and Boltalina O. 2005. Surface transfer doping of diamond by fullerene. *Diamond and Related Materials*. 14(3-7): 451-458.
- [11] Strobel P., Ristein J., Ley L., Seppelt K., Goldt I. V. and Boltalina O. 2006. Surface conductivity induced by fullerenes on diamond: Passivation and thermal stability. *Diamond and Related Materials*. 15 (4-8): 720-724.
- [12] Heremans F., Fuchs G., Wang C., Hanson R. and Awschalom D. 2009. Generation and transport of photoexcited electrons in a single-crystal diamond. *Applied Physics Letters*. 94 (15): 152102-152104.
- [13] Edmonds M., Pakes C., Mammadov S., Zhang W., Tadich A., Ristein J. and Ley L. 2011. Work function, band bending, and electron affinity in surface conducting (100) diamond. *Physica Status Solidi (a)*. 208(9): 2062-2066.